

OPTIMIZATION OF A NOVEL LATERAL DEFORMABLE NEMS ZERO-ORDER GRATINGS: ANOMALOUS DIFFRACTION STUDIED BY 3-D FDTD METHOD

Chen Wang¹, Jian Bai^{1,*}, Qian-Bo Lu¹ and Guo-Guang Yang¹

1 State Key Laboratory of Modern Optical Instrumentation, Yuquan Campus of Zhejiang University No.3 Building,
No. 38, Zheda Road, Xihu District, Hangzhou 310027, China

* Corresponding author: bai@zju.edu.cn

Abstract:

This paper discusses the analysis and optimization of a novel optomechanical zeroth-order grating transducer based on an anomalous diffraction phenomenon, namely Wood's type anomaly, in which tiny changes in the displacement of the nanostructured grating elements lead to a dramatic increase or decrease of the optical reflection amplitude. With this special feature, this structure is an ideal sensor component to observe very small displacement. This device is very sensitive to wavelength, the period and the width of the grating. Here, we analyze the performance of the structure with different parameters and optimize the original structure corresponding to 850nm through 3-D Finite Difference Time Domain method (FDTD). Simulation demonstrates the new structure is of higher sensitivity and signal strength, namely extinction ratio. Moreover, in order to enlarge the tiniest size of the original structure which is closely related to the incident wavelength, we change the wavelength to longer ones, e.g. 1053nm, 1310nm, 1530nm. The calculation predicts the optimized structure designs of those wavelengths are of performance similar to the original one's but much less strict demand for processing precision, which makes it possible to be fabricated with current surface micromachining processing similar to that used for the fabrication of polysilicon MEMS. Besides, structures of several visible incident wavelengths, such as 532nm, 632.8nm, 670nm, 753nm, are also analyzed and optimized, which gives great convenience to the installation and calibration of such device as well as observation of its performance. All the calculated data enable us to apply the structure into fields required for different sensitivities with different grating designs and thus broaden the further usage of such novel structure, as structures of different parameters are of different sensitivities and signal strengths.

Keywords: Nanoelectromechanical systems (NEMS), grating transducer, 3-D Finite Difference Time Domain method(FDTD), microelectromechanical systems (MEMS), optical resonant detections.

1. INTRODUCTION

Wood's anomaly was first observed by Dr. Wood in 1902 in his research concerning reflection gratings, which manifests itself as tremendous increase or decrease in the intensity of several grating orders due to small variation of the physical parameters, e.g. the wavelength and can not be explained with ordinary theories of gratings [1]. Since then,

this phenomenon had become the focus of numerous research work and been studied theoretically and experimentally in detail [2-3]. Nowadays, those theories concerning Wood's anomaly can be applied into practical use with precise design and fabrication of gratings in sub-wavelength dimension., thanks to the rapid development of computer simulation software, such as 3-D Finite Difference Time Domain (FDTD) method and microelectromechanical system (MEMS) technology. Typical examples of such application are optical filter [4], guided-mode resonant filter (GMRF) [5-6], high speed laser scanning[7]. Recently, Dustin presented a novel grating design based on Wood's anomaly and demonstrated his work with rigorous analysis [8], experimental test [9] as well as following application in an optical accelerometer [10-11]. This device gives out rapid variation of reflective intensity with small lateral displacement in nanometer scale and is quite sensitive to incident wavelength, which makes it very suitable for small displacement detection and beam-splitting switch. However the setting of grating parameters as well as incident light is absent in the discussion in Dustin's work, which is crucial to the occurrence of Wood's anomaly and performance of the corresponding transducer. In this paper, we analyze the influence of different parameters, such as period, incident wavelength, on the performance of the structures through FDTD method. The simulation result gives out the respective influence of those parameters and the optimized structure designs for different wavelengths. With this knowledge, the original structure design corresponding to 850nm has been optimized and resulted into a new design of higher sensitivity and signal strength, namely extinction ratio. Besides, optimized structure design for longer wavelengths are calculated for the enlargement of the tiny size of original design and shorter visible wavelengths are considered for the convenience of the installation and calibration of such device as well as observation of its performance. All calculated data enable us to apply the structure into fields required for different sensitivities and dynamic ranges with different grating designs and thus broaden the further usage of such novel structure.

2. DEVICE DESIGN

This device consists of six separated regions: upper grating region, an air gap, lower grating region, an antireflective coating, a silicon dioxide layer and a substrate, as shown in Figure 1. The two-layer optical gratings are defined in two vertically offset silicon layers suspended in air and separated by an air gap. The upper grating is design to be moved laterally, while the bottom grating is attached to the silicon substrate which are first oxidized to produce an 0.6 μm of silicon dioxide and then coated with an 0.8 μm of low stress silicon nitride to form an antireflective layers. The bottom three layers of the substrate can be removed instead, which leaves two layers of gratings completely suspended with no boundaries on either side and results in the same reflective intensity as that mentioned here. All of the setting and simulation are carried out on a computer with 3-D Finite Difference Time Domain (FDTD) software, as ordinary analytical approximation is not precise enough to calculate the electromagnetic fields of such small device whose period is in sub-wavelength scale. FDTD method is an efficient method to analyze the characteristics of wavelength scale complex structures with ultraviolet, visible and infrared radiation based on Maxwell's equation.

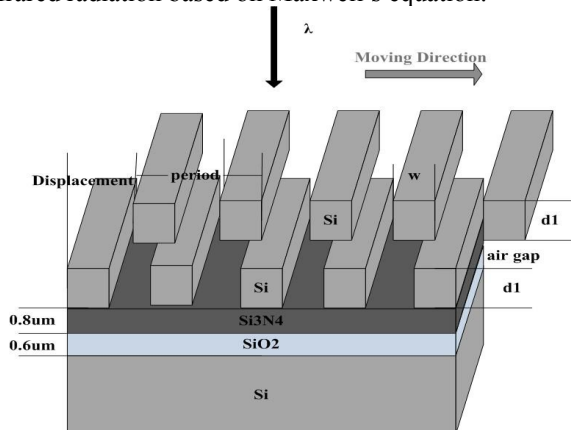


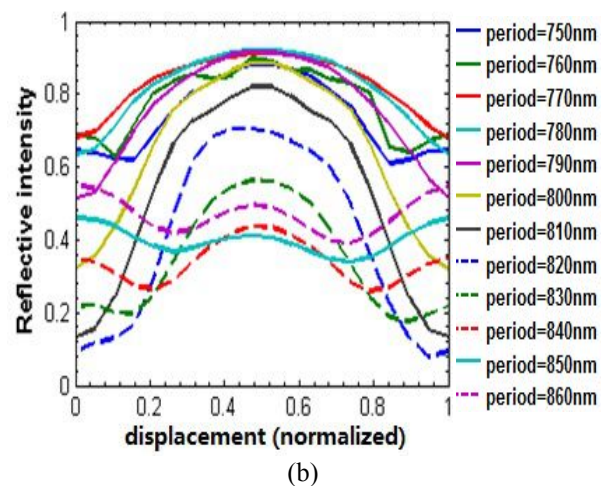
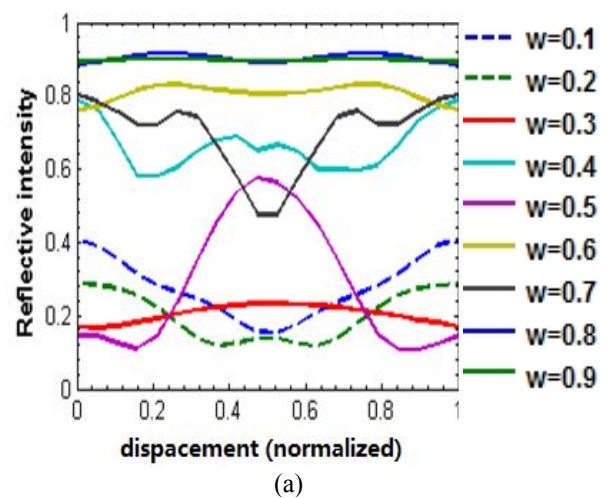
Fig. 1: Cross section of the laterally deformable optical NEMS grating transducer, with relevant parameters shown. The reflective index of the antireflective layer and silicon substrate is set as $n = 2.0$ and $3.86 - i0.02$ respectively. The thickness of antireflective layer and silicon dioxide is 0.8 μm and 0.6 μm respectively. For all calculation here, displacement is the relative lateral displacement between two layers of gratings, $d1$ is the thickness of gratings, w is the duty ratio of grating element, period is the period of grating. The two layers of gratings are set identically and separated with an air gap.

3. SIMULATION METHOD AND RESULT

The performance of the device is evaluated in two aspects, namely the extinction ratio and slope of the reflective curve as function of the lateral displacement (displacement). The curve of a structure with large slope and extinction ratio is considered as an optimal design, as large slope indicates better sensitivity and large extinction ratio indicates

dramatic difference of signal received by photoelectric detectors. Besides, large extinction ratio is also a desire feature for its application in optical switchers or displays.

For this work, we concentrate on analysis and optimization of structures under incident light of 850nm mentioned in Dustin's work. First, we find out four major parameters, namely period, duty ratio of a grating element, thickness of each layer of gratings, air gap, which impose great influence on the performance of the device, by checking the corresponding performance of the device with changes of each parameter. Figure 2 shows the reflective intensity of a TE-polarized beam at normal incidence as a function of the lateral displacement (displacement). Ten different duty ratios (w), ten different air gaps, four different periods as well as ten different thicknesses of gratings ($d1$), are considered respectively, representing their independent influences on performance of the device.



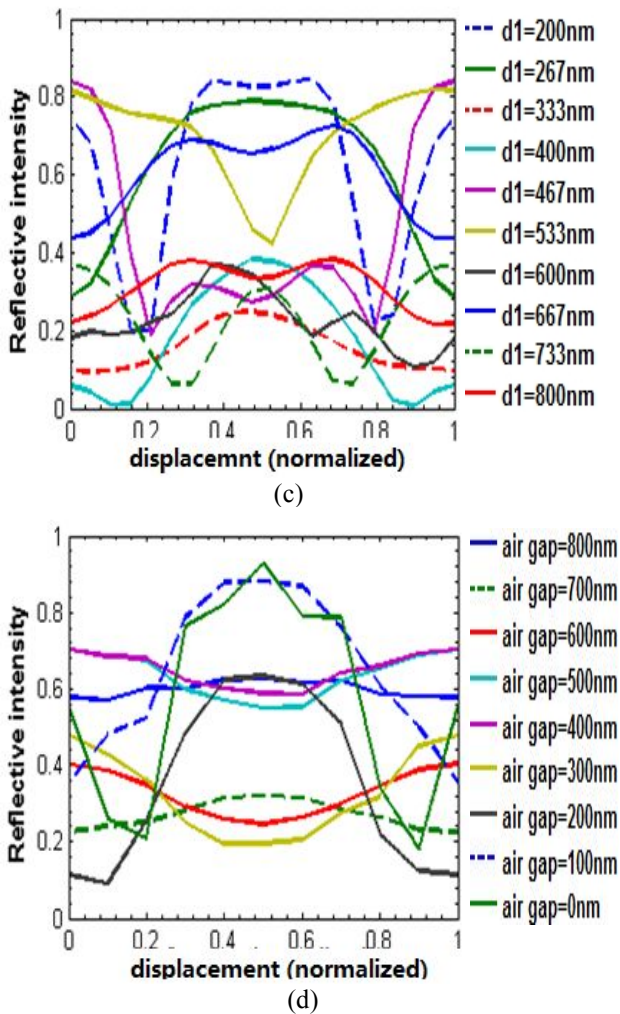
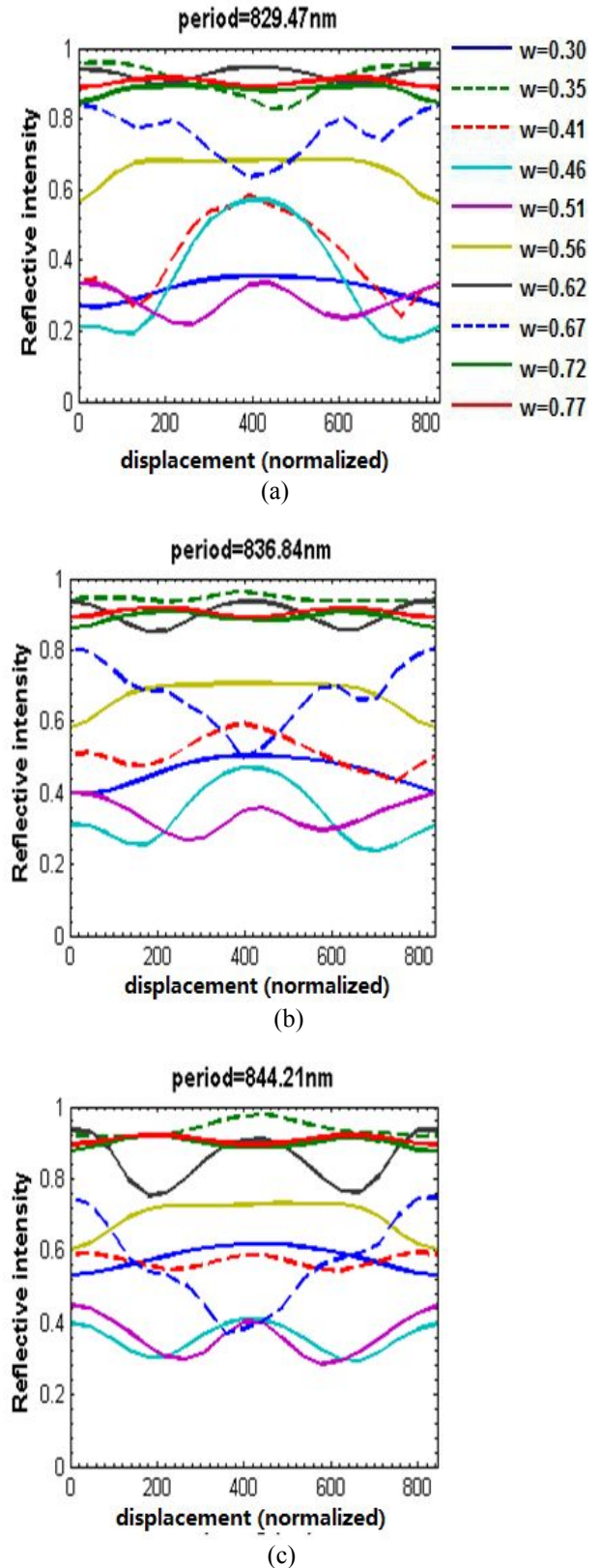


Fig. 2: (a) TE mode reflectance with variation of the lateral displacement (displacement) for three different duty ratios (w). The value of other three grating parameters are held constant, namely period = 820nm, the thicknesses of gratings ($d1$) = 300nm, air gap = 193nm. (b) TE mode reflectance with variation of the lateral displacement (displacement) for three different periods. The value of other three grating parameters are held constant, duty ratio (w) = 0.5, the thicknesses of gratings ($d1$) = 300nm, air gap = 193nm. (c) TE mode reflectance with variation of the lateral displacement (displacement) for three different thicknesses of gratings ($d1$). The value of other three grating parameters are held constant, namely period = 820nm, duty ratio (w) = 0.5, air gap = 193nm. (d) TE mode reflectance with variation of the lateral displacement (displacement) for three different air gap. The value of other three grating parameters are held constant, namely period = 820nm, the thicknesses of gratings ($d1$) = 300nm, duty ratio (w) = 0.5.

Figure 2 shows the optimal value for each parameter when they are modified independently. However, when set with these values simultaneously, the structure does not give out the desired performance, on the contrary whose extinction ratio is 42.37% and slop is 0.10%/nm. This paradox indicates these parameters are interdependent and thus have to be modified with consideration of their mutual

influence to get the optimal values. Thus, two parameters are considered and changed as a group each time while the rest two parameters are held constant, since we are capable to manually select and tell the optimal values from at most 3-D chart. Part of the data are shown in Figure 3 and Figure 4.



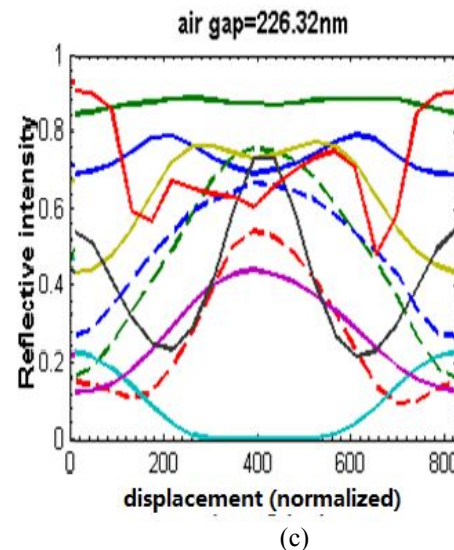
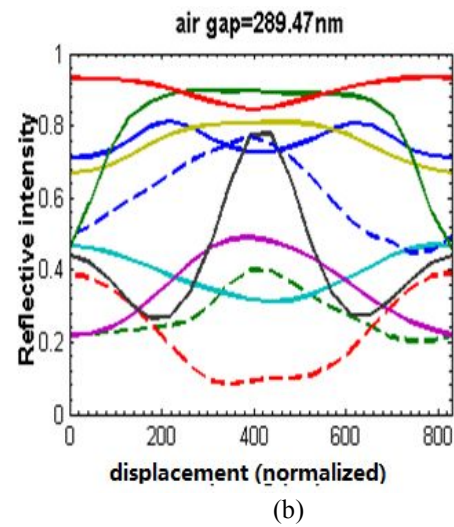
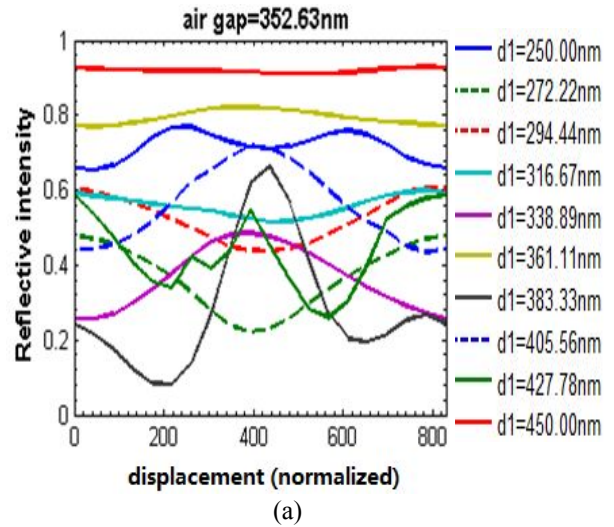
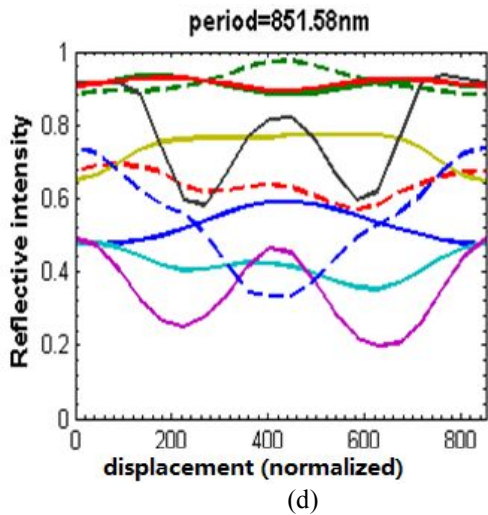


Fig. 3: (a) TE mode reflectance with variation of the lateral displacement (displacement) for three different duty ratios (w). The value of other three grating parameters are held constant, namely period = 820nm, the thicknesses of gratings (d_1) = 300nm, air gap = 193nm. (b) TE mode reflectance with variation of the lateral displacement (displacement) for three different periods. The value of other three grating parameters are held constant, duty ratio (w) = 0.5, the thicknesses of gratings (d_1) = 300nm, air gap = 193nm. (c) TE mode reflectance with variation of the lateral displacement (displacement) for three different thicknesses of gratings (d_1). The value of other three grating parameters are held constant, namely period = 820nm, duty ratio (w) = 0.5, air gap = 193nm. (d) TE mode reflectance with variation of the lateral displacement (displacement) for three different air gap. The value of other three grating parameters are held constant, namely period = 820nm, the thicknesses of gratings (d_1) = 300nm, duty ratio (w) = 0.5.

Figure 3 shows the reflective curve as a function of lateral displacement (displacement) with two parameters changed as a group. The reflective curve as a function of lateral displacement (displacement) with simultaneous alteration of twenty different periods and duty ratios (w). The other two parameters, namely air gap, the thickness of gratings (d_1) are held as 193nm and 300nm respectively. Four out of twenty different periods and ten out of twenty duty ratios are shown. (a) Period is set 829nm while ten duty ratios (w) are considered. (b) Period is set 837nm while ten duty ratios (w) are considered. (c) Period is set 844nm while ten duty ratios (w) are considered. (d) Period is set 852nm while ten duty ratios (w) are considered.

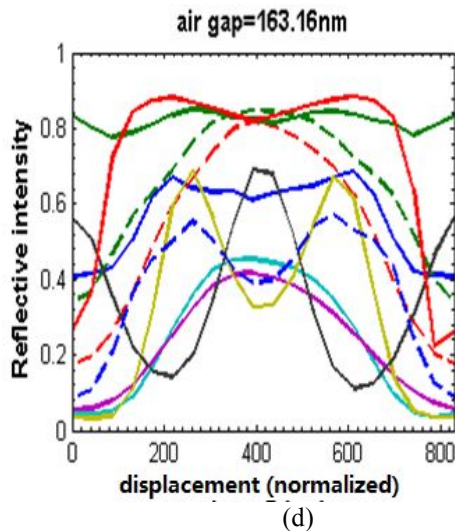


Fig. 4: The reflective curve as a function of lateral displacement (displacement) with simultaneous alteration of forty different air gaps, ten different thicknesses of gratings (d1). The other two parameters, namely period and duty ratio (w), are held as 829nm and 0.46 respectively, which are the optimal values from simulation in Figure 3. Four out of forty different air gaps and ten duty ratios are shown. (a) Air gap is set 353nm while ten the thicknesses of gratings (d1) are considered. (b) Air gap is set 289nm while ten the thicknesses of gratings (d1) are considered. (c) Air gap is set 226nm while ten the thicknesses of gratings (d1) are considered. (d) Air gap is set 163nm while ten the thicknesses of gratings (d1) are considered.

To better improve the sensitivity and extinction ratio of the device, it is necessary to write a computer program to calculate the four parameters simultaneously and change each value according to corresponding influence of three other parameters. These can be easily done with Gradient optimization algorithm [12-14]. Gradient optimization algorithm is an efficient method to search for optimal values for structure design in case where multiple variables are interdependent. Gradient descent is based on the observation that if the multivariable function $F(x)$ is defined and differentiable in a neighborhood of a point A, then $F(x)$ decreases fastest if one goes from A in the direction of the negative gradient of F at A [15]. However, this optimization algorithm will get stuck into local extreme points from time to time, if the partial derivative of function of merit for each parameters has too many zero points. It is especially true when the four parameters here are considered, presenting a result far cry from desired value.

Given the situation mentioned above, we change the optimization algorithm to Particle Swarm Optimization (PSO) algorithm, which is a population based stochastic optimization technique, inspired by the social behavior of flocks of birds or schools of fish [16-17], and has widely been used for various kinds of design optimization problems including nanophotonic design [18]. Simulation result indicates the optimal values for period, duty ratio (w), thickness of gratings (d1), air gap are 775nm, 0.529, 519nm, 612nm respectively. Figure 5 shows the reflective curve as

function of lateral displacement (displacement) of structure with parameters set as those optimal values. For this particular geometry, the extinction ratio is 85.69% and the slop is 0.22%/nm which are higher than those of the original structure mentioned in Dustin's work.

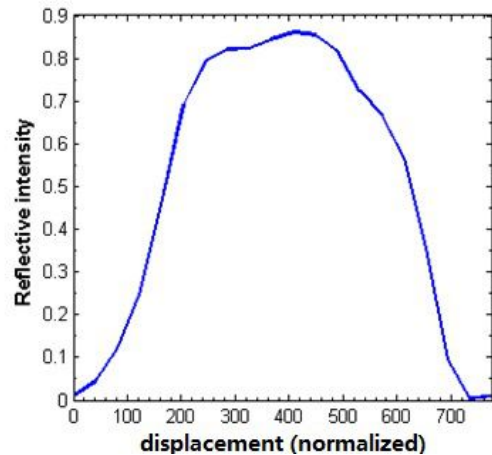


Fig. 5: The reflective curve as function of the lateral displacement (displacement) of structure with period, duty ratio (w), thickness of gratings (d1), air gap set as 775nm, 0.529, 519nm, 612nm respectively.

In order to enlarge the tiniest size of the structure design, which is closely related to the wavelength of incident light, we replace the incident light of 850nm with ones of longer wavelengths, such as 1053nm, 1310nm, 1530nm, shown in Table 1. From Table 1, we can tell the optimal value of the period and the thickness of gratings (d1) rises with the increase of incident wavelength. It is especially true when it comes to the optimized structure design for incident wavelength of 1530nm, in which its period, the thickness of gratings (d1) are almost two times larger than that for incident wavelength of 850nm, meaning much less strict demand of process precision and its extinction ratio, namely 96%, is 11% higher than that for incident wavelength of 850nm.

Table 1: Chart concerning optimal values of period, period, duty ratio (w), thickness of gratings (d1) and air gap for structure under illumination of different wavelength longer than 850nm, namely 1053nm, 1310nm, 1530nm.

Incident wavelength (nm)	1530	1310	1053	850
Period (nm)	1456	1351	970	775
Duty ratio (w)	0.530	0.300	0.300	0.529
Thickness of gratings (d1) (nm)	960	1276	1009	519
Air gap (nm)	200	200	200	612
Extinction ratio (%)	96.189	84.170	83.945	85.687
Slop (%/nm)	0.165	0.099	0.183	0.221

Since the incident light mentioned above is invisible, optimized structure designs for shorter wavelengths, such as 753nm, 670nm, 632.8nm, 532nm, are also considered and calculated, shown in Table 2, which will provide great convenience for the installation and calibration of such device as well as observation of its performance.

Table 2: Chart concerning optimal values of period, period, duty ratio (w), thickness of gratings (d1) and air gap for structure under illumination of different wavelength shorter than 850nm, namely 753nm, 670nm, 632.8nm, 532nm.

Incident wavelength (nm)	850	753	670	632.8	532
Period (nm)	775	668	630	558	520
Duty ratio (w)	0.529	0.425	0.490	0.591	0.390
Thickness of gratings (d1) (nm)	519	700	132	114	102
Air gap (nm)	612	200	200	197	100
Extinction ratio (%)	85.687	76.629	79.941	76.273	76.580
Slop (%/nm)	0.221	0.271	0.302	0.289	0.491

4. CONCLUSIONS

In conclusion, this work have analyzed and optimized a novel laterally deformable optical NEMS grating transducer that can be modified into ones with different extinction ratios and sensitivities according to different demand. From Table 1 , optimal structures for incident wavelengths, namely 1530nm, 1310nm, 1053nm and 850nm, give out stronger signal, namely larger extinction ratio and demand less strict process precision while optimal structures for incident wavelengths, namely 753nm, 632.8nm and 532nm, are preferred to detect small displacement and the light is visible. In addition, optimal structures for visible incident wavelengths, namely 670nm, reach a balance between the sensitivity and extinction ratio. Moreover, Table 1 indicates the general relationship among incident wavelength, period, duty ratio (w), thickness of grating (d1), air gap for optimal design, in which air gap generally need to be set as smaller than 200nm, the difference between period and incident wavelength generally is between 40nm and 90nm, duty ratio (w) generally need to be set as a value between 0.3 and 0.6. Besides, the largest extinction ratio for structures with incident wavelength smaller than 440nm can not be higher than 40%. Optimizing the device with finer sweeping interval, as well as considering other subordinate factors and simulating the structure with plane wave rather than a focused beam, could further increase its sensitivity.

Currently research involves a more detail quantificational discussion of the interdependent relationship among the five

factors which will enable us to modify the structure for custom usage more conveniently. Furthermore, we are planning to test the simulation result experimentally and apply different designs into various detection areas, such as microgravity detection for resource exploration and other inertial sensors, as well as a modulator for optical switching, since this device is very sensitive to wavelength.

ACKNOWLEDGEMENTS

This work was supported by National Science Foundation of China.

REFERENCES

- [1] Wood, R. W. "Anomalous diffraction gratings." *Physical Review*, vol.48(12), pp. 928, 1935.
- [2] Hessel, A., and A. A. Oliner. "A new theory of Wood's anomalies on optical gratings." *Applied Optics*, vol.4(10), 1275-1297, 1965.
- [3] Peter, Thorsten, Ralf Bräuer, and Olof Bryngdahl. "Occurrence of resonance anomalies for index modulated gratings." *Optics communications*, vol.139(4), pp. 177-181, 1997.
- [4] Magnusson, R., and S. S. Wang. "New principle for optical filters." *Applied physics letters*, vol.61(9), 1022-1024, 1992.
- [5] Feng, Li, et al. "Experimental study of the generation of Laguerre-Gaussian beam using a computer-generated amplitude grating." *Acta Physica Sinica*, vol.57, pp. 860-866, 2008.
- [6] Zhi-Hua, Wang, et al. "The correction of short-range Mie scattering laser lidar returns based on the Gaussian character of laser beam." *Acta Physica Sinica*, vol.55(6), pp. 3188-3192, 2006.
- [7] Du, Yu, et al. "High speed laser scanning using MEMS driven in-plane vibratory grating: Design, modeling and fabrication." *Sensors and Actuators A: Physical*, vol.156(1), pp. 134-144, 2009.
- [8] Carr, Dustin W., J. P. Sullivan, and T. A. Friedmann. "Laterally deformable nanomechanical zeroth-order gratings: anomalous diffraction studied by rigorous coupled-wave analysis." *Optics letters*, vol.28(18), pp. 1636-1638, 2003.
- [9] Carr, Dustin W., et al. "Measurement of a laterally deformable optical MEMS grating transducer." *Proc. SPIE*, vol.5346, pp. 56-63, 2004.
- [10] Keeler, Bianca E., Gregory R. Bogart, and Dustin W. Carr. "Laterally deformable optical NEMS grating transducers for inertial sensing applications." *Proc. SPIE*, vol.5592, pp. 306-312, 2005.
- [11] Keeler, Bianca EN, et al. "Experimental demonstration of a laterally deformable optical nanoelectromechanical system grating transducer." *Optics letters*, vol.29(111), pp. 182-1184, 2004.
- [12] Polak, Elijah. [Optimization: algorithms and consistent approximations], Springer-Verlag Publishers, New York, 1997.
- [13] Watrous, Raymond L. "Learning algorithms for connectionist networks: Applied gradient methods of nonlinear optimization." *Technical Reports (CIS)*, vol.597, 1988.
- [14] Avriel, Mordecai, [Nonlinear programming: analysis and methods], Courier Dover Publications, 2012.

- [15] Snyman, Jan, [Practical mathematical optimization: an introduction to basic optimization theory and classical and new gradient-based algorithms], Springer, 2005.
- [16] J. Robinson and Y. Rahmat-Samii, "Particle swarm optimization in Electromagnetics," IEEE Trans. Antennas and Propagat, vol.52, pp. 397 - 407, 2004.
- [17] K. E. Parsopoulo and M N. Vrahatis, [Particle swarm optimization and intelligence : advances and applications], Hershey, pp. 1-4, 2010.
- [18] J. Pond and M. Kawano, "Virtual prototyping and optimization of novel solar cell designs," Proc. SPIE, vol.7750, pp. 775028-775028, 2010.